

Partial Discharge Behavior of Typical Defects in Power Equipment under Multilevel Staircase Voltage

Zang, Yiming; Niasar, Mohamad Ghaffarian; Ganeshpure, Dhanashree Ashok; Qian, Yong; Sheng, Gehao; Jiang, Xiuchen; Vaessen, Peter

DOI

[10.1109/TDEI.2022.3185567](https://doi.org/10.1109/TDEI.2022.3185567)

Publication date

2022

Document Version

Accepted author manuscript

Published in

IEEE Transactions on Dielectrics and Electrical Insulation

Citation (APA)

Zang, Y., Niasar, M. G., Ganeshpure, D. A., Qian, Y., Sheng, G., Jiang, X., & Vaessen, P. (2022). Partial Discharge Behavior of Typical Defects in Power Equipment under Multilevel Staircase Voltage. *IEEE Transactions on Dielectrics and Electrical Insulation*, 29(4), 1563-1573. <https://doi.org/10.1109/TDEI.2022.3185567>

Important note

To cite this publication, please use the final published version (if applicable). Please check the document version above.

Copyright

Other than for strictly personal use, it is not permitted to download, forward or distribute the text or part of it, without the consent of the author(s) and/or copyright holder(s), unless the work is under an open content license such as Creative Commons.

Takedown policy

Please contact us and provide details if you believe this document breaches copyrights. We will remove access to the work immediately and investigate your claim.

Partial Discharge Behavior of Typical Defects in Power Equipment under Multilevel Staircase Voltage

Yiming Zang, Mohamad Ghaffarian Niasar, Dhanashree Ashok Ganeshpure, *Student Member, IEEE*, Yong Qian, Gehao Sheng, *Member, IEEE*, Xiuchen Jiang and Peter Vaessen, *Member, IEEE*

Abstract—With the widespread application of power electronic switching technology, power equipment is facing new electrical stresses brought about by multilevel staircase voltages during testing and operation. Therefore, the partial discharge (PD) behavior of 5 typical defects in power equipment under the staircase waveform needs to be investigated. This paper mainly analyses the phase-resolved partial discharge (PRPD) pattern and pulse repetition rate of 5 typical defects under sinusoidal voltage and multilevel staircase voltage with different number of levels. Also, the PD behavior under staircase voltage with different step responses are investigated. By analyzing the reasons behind the PD behavior between different cases, the PD characteristics and the transformation of PRPD patterns under different staircase voltages are obtained. Moreover, this research finds that the sensitivity of different defects to the staircase voltage is different. These results provide experimental and theoretical support for the testing and diagnosis of PD under new electrical stress present in the future flexible electric grid.

Index Terms—partial discharge (PD) mechanism, modular multilevel converter (MMC), multilevel staircase voltage, typical defects, phase-resolved partial discharge (PRPD).

I. INTRODUCTION

With the development of renewable energy and smart grid, a large number of power equipment integrated with power electronics and semiconductor switching devices have been widely used for energy conversion and transmission [1]. Under these circumstances above, power electronics based technologies such as modular multilevel converter (MMC) and pulse width modulated inverters are gradually accepted in power applications [2]. However, the switching operation of power electronic devices introduce new electrical stresses to power equipment, such as multilevel staircase waveform voltage [3]. The appearance of the multilevel staircase waveform voltage will pose a new challenge to the insulation state evaluation, which are typically assessed through the analysis of partial discharge (PD) [4].

PD detection is one of the most important ways to pre-protect the power equipment by monitoring discharge information of

insulation defects, which is an enabler to the safe operation of the power system [5, 6]. Since the PD transition under different voltage waveform will affect the characteristic and criteria of the status diagnosis [7], studying the difference of PD behavior under staircase waveform and traditional sinusoidal waveform is crucial to guide PD detection under the new electric stress in high voltage (HV) power equipment, which is a new research direction.

At present, some scholars have carried out the research of PD under multilevel staircase voltage. The simulation and effects of discharge condition on PD behavior in voids under square voltages has been investigated [8,9]. Reference [10] studies the PD characteristics of low voltage motors under repetitive surge voltages to guide the motor's state detection. Reference [11] reports the PD behavior of twisted pairs under two-level pulse width modulator voltage, which finds that the PD distribution has a certain correlation with the pulse width. It is concluded in Reference [12] that square-wave voltage can influence the pulse repetition rate and evolution process of PD in wide bandgap power devices. Also, the inverter parameters and the number of levels (3-, 5- and 9-level) in PWM voltage has been proven to change the amplitude, inception voltage and phase distribution of PD in rotating machines [13-15]. As it is now, it implies that the old PD measurement method does not work for new type of stress. In order to better understand PD behavior under this new type of electric stress, some researchers have developed an arbitrary waveform HV source to test the PD behavior of a needle defect under staircase waveforms [16]. There is also further research work ongoing to develop high voltage power electronics based test sources to be able to test future power components under realistic in-service electric stress [17]. However, the available information on literature is not enough to support testing and detection under new electrical stress, and lacks the PD behavior analysis of the typical defects that have been extensively observed during the manufacturing and operation of power equipment, such as surface defect, floating defect, internal defect, etc. Furthermore, there is also less research on the staircase waveform with more than 10 levels, which is more likely to occur in practical operation.

Therefore, in order to better adapt to the uncertain effects of the new electrical stress and to guide the PD detection, the PD behavior and mechanism under staircase waveforms were done and give findings. In this work, five typical PD defects are tested under conventional sinusoidal voltage and staircase-based sinusoidal voltages of different levels (5- to 99-level), which is helpful to understand the effect of different waveforms. Taking the PD under the sinusoidal voltage as a reference of

This work was supported in part by the National Natural Science Foundation of China under Grant No. 62075045.

Yiming Zang, Yong Qian (*corresponding author*), Gehao Sheng and Xiuchen Jiang are with the Department of Electrical Engineering, Shanghai Jiao Tong University, Shanghai 200240, China (e-mail: zangyiming@sjtu.edu.cn; qian_yong@sjtu.edu.cn; shenghe@sjtu.edu.cn; xcjiang@sjtu.edu.cn).

Mohamad Ghaffarian Niasar, Dhanashree Ashok Ganeshpure and Peter Vaessen are with the Delft University of Technology, Mekelweg 4, 2628 CD, Delft, Netherlands (e-mail: M.GhaffarianNiasar@tudelft.nl; D.A.Ganeshpure@tudelft.nl; P.T.M.Vaessen@tudelft.nl).

comparison, the phase-resolved partial discharge (PRPD) pattern, average phase similarity, the effect of step response and the pulses repetition rate (PRR) under each defect are all investigated. Regarding the PD phenomenon, the experiments in this paper indicate that the influence of staircase voltage with different levels on 5 typical defects. Through the analysis of these PD behavior under different conditions, the results can provide a theoretical reference for PD testing and diagnostics under new electrical stress in the future.

II. EXPERIMENTAL SETUP AND TEST PROCEDURES

In order to study the influence of the staircase waveform voltage on PD occurrence, five typical PD defects are selected for experimental research in this paper, as shown in Fig. 1. Under the staircase voltage, we did the PD experiments in SF₆ for needle defect, floating defect, particle defect, surface defect and in air for internal defect. The radius of the SF₆ gas chamber used for the experiment is 25mm and the height is 65mm. The pressure of SF₆ is 0.2Mpa (abs). The needle tip radius is 250μm. The radius of the particle in the free particle defect is 2mm. The thickness of the dielectric in the surface defect is 3mm and the radius of the metal electrode is 5mm. The radius of the cylindrical gas inclusion in the internal defect is 2.5mm and the height is 0.7mm.

Fig. 2 illustrates the entire corona-free PD setup. The programmable waveform generator (Tektronix AFG3252C) is used to generate staircase waveform of different levels. A Trek 30/20A HV amplifier is connected to the output of the waveform generator and act as the voltage source with frequency of 50Hz. The experimental peak voltage for the needle defect, floating defect, particle defect, surface defect and internal defect are 14kV, 13kV, 17kV, 25kV, 5kV respectively. PD signals are detected by using a high-frequency current transformer (Techimp HFCT), which has a gain of 9.1 mV/mA and 40kHz-130MHz bandwidth. The Picoscope 6.0 Oscilloscope is used for collecting the PD data with 1.25GS/s sampling rate. A low coupling capacitor with 500pF is put into the setup to ensure the fast step response and high-frequency path for PD signal. Since this paper requires applying different voltages to different defects and varying the number of levels of the staircase voltage, therefore, the voltage gradient is not a completely constant value. By measurement, the voltage gradient is kept between 150V/μs and 170V/μs in this paper. This voltage gradient is relative slower than the real values generated by modern voltage inverters. According to the existing research, the rise time of the voltage can affect the PD amplitude, PD inception voltage, and frequency components of the PD [18], but since the main purpose of this paper is to study the PD phase distribution behavior and the reason behind the PD characteristics, therefore the used voltage gradient is acceptable. Although various voltage rise times affect the PRPD patterns, but the intrinsic logic can be explained by the theory in this paper. We will use a medium voltage MMC with shorter rise times to extend this investigation in future work. In this paper, the same step response of the circuit is used for the analysis of PRPD patterns for different defects in Section III,

which can ensure the reasonableness of the comparative analysis.

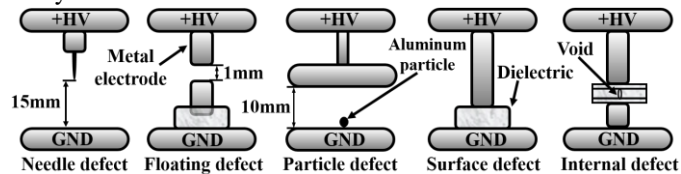


Fig. 1. Five typical PD defects.

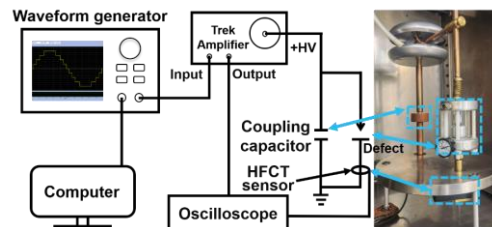


Fig. 2. Schematic diagram and actual view of the experiment setup.

Based on the setup, the test work in this paper mainly includes three parts:

(1) For each type of defect, PD experiments are carried out under the voltage waveform of 5-, 9-, 13-, 25-, 39-, 59-, 79-, 99-level staircase waveforms and the sinusoidal waveform. 2000 PD pulses are collected to plot the PRPD patterns.

(2) Increasing the value of the coupling capacitor makes the step response of the staircase waveform slower.

(3) The average PRR of each defect under the above-mentioned waveforms are calculated. To calculate the PRR, we record the time required while collecting the same number of PD pulses for each PD defect under different voltage waveforms, thus calculating the number of PD pulses are collected per second (PRR value). Each case is tested 10 times, and the average value is calculated. In order to allow the insulation to be restored without affecting the results of the next test, the interval between each experimental acquisition is 10 minutes.

III. PRPD PATTERN AND DISCHARGE BEHAVIOR UNDER DIFFERENT DEFECTS

This section shows the PRPD patterns and discharge behavior of 5 defects under the traditional sinusoidal waveform and the staircase waveforms with different number of levels. According to the responsivity of different defects to the staircase voltage, the number of levels that are representative are selected for explanation.

A. Needle defect

For the needle defect under the same applied voltage, the complete PRPD patterns and partial enlarged patterns of sinusoidal waveform and staircase waveforms with 5-, 9-, 13-, 25- and 39-levels are shown in Fig. 3. The amplitude of the ordinate in Fig. 3 represents the oscilloscope acquisition value, and the red waveform is the actual shape of waveform. It can be seen from Fig. 3 that the PDs of the needle defect are all distributed near the peak of negative cycle under different voltage waveforms, but the shape changes.

For the staircase waveform, as the number of levels increases, the shape of the PRPD pattern gradually changes from a square to sinusoidal PD pattern. The phase distribution range of PD is also reduced from 81.8° (5-level) to 60.7° (9-level), and then gradually expands to about 69.8° (39-level), which is almost similar to a sinusoidal waveform. This phenomenon is different from the PD at multilevel inverter voltage [4, 15]. Each level of the staircase voltage is a DC component, while each level in the multilevel inverter voltage is composed of some square waveforms. Therefore, PDs at multilevel inverter voltage are grid-like in distribution at each level, while the portion of the staircase voltage that above the level of PD inception voltage (PDIV) causes PD similar to those at DC voltage. Due to the effect of voltage steps, it can be seen from the PRPD density that there is a denser discharge in the area close to the rising edge of the staircase waveform at 5-level and 9-level, while it gradually returns to a dense discharge distribution in the middle and sparse at both ends from 25-level and beyond. According to the speculation, this is because of the delay effect of electric field caused by space charge. This paper takes the 5-level staircase waveform as an example, and the explanation given in the next paragraphs is also applicable to different levels, as shown in Fig. 4.

The occurrence of PD requires sufficient electric field and presence of initial electrons to cause avalanches. The delayed supply of initial electrons is the main reason for the randomness of PD. Therefore, the PD occurrence depends on the fact that the electric field in the defect \vec{E}_n need to be higher than the minimum PD inception field E_{min} . During the discharge process, \vec{E}_n is formed by the resultant of the electric field \vec{E}_a generated by the external voltage and the electric field \vec{E}_s generated by the accumulation of space charges, as it results from:

$$\vec{E}_n = \vec{E}_a + \vec{E}_s \quad (1)$$

For the corona discharge, the E_{min} of the positive and negative cycles are different, denoted as E_{min+} and E_{min-} respectively. The conditions for PD can be expressed as:

$$\begin{cases} E_p > E_{min+}, & 0^\circ < phase < 180^\circ \\ E_p > E_{min-}, & 180^\circ < phase < 360^\circ \end{cases} \quad (2)$$

where E_p represents the field value of \vec{E}_n near the tip of the needle. Since the E_{min+} of the corona discharge is higher than the E_{min-} , the PD mainly occurs in the negative half cycle first and the PD of the positive half cycle does not occur unless the applied voltage is sufficiently high. Fig. 4 shows a schematic diagram of the electric field that changes under DC component of the voltage [19].

When the electric field strength near the needle tip meets the PD condition in (2), PD will occur. When a PD occurs in the negative half-cycle, the positive charge around the needle tip will move into the needle tip, and a large amount of negative charge remains near the needle tip outside. Under the continuous DC voltage component of the staircase voltage, the electrons between the defect gap move to the ground electrode to recover the electric field near the needle tip. When the field strength near the tip reaches E_{min} , PD occurs again. However, when the first PD occurs in a half-cycle, there is no accumulation of negative space charges in the defect space.

Because the time between two half cycle is sufficiently large compared to the time needed for the charges to pass the gap. As the number of discharges in this half-cycle increases, more electrons can accumulate in the space between the needle and ground. Due to the reverse force generated by the accumulation of electrons, this will gradually increase the total electric field produced by the negative space charges after each PD, thereby extending the recovery time of the electric field near the needle tip. For a clearer description, the gradual delay process of the PD time interval is illustrated it in Fig. 4(a). Therefore, in the DC stage of the staircase waveform, the interval time of each PD will gradually become longer, as shown in Fig. 4(b). Due to this, the discharge near the rising edge is denser, and then gradually sparse, as shown in Fig. 3(b) and (c). In addition, when the number of levels of the staircase waveform increases, the amplitude of the rising voltage of each level becomes smaller. When the voltage just exceeds PDIV a little, it takes longer time between two consecutive PDs under this level. As the voltage level gradually increases to the peak value, the background electric field in the defect becomes stronger, making the time interval between two consecutive PDs shorter. Therefore, the PD density is greater at levels near the peak.

What's more, as the amplitude difference between the multiple levels gradually decreases, it can be observed that the PD pattern of a 39-level staircase waveform is basically similar to that of sine waveform in Fig. 3(f).

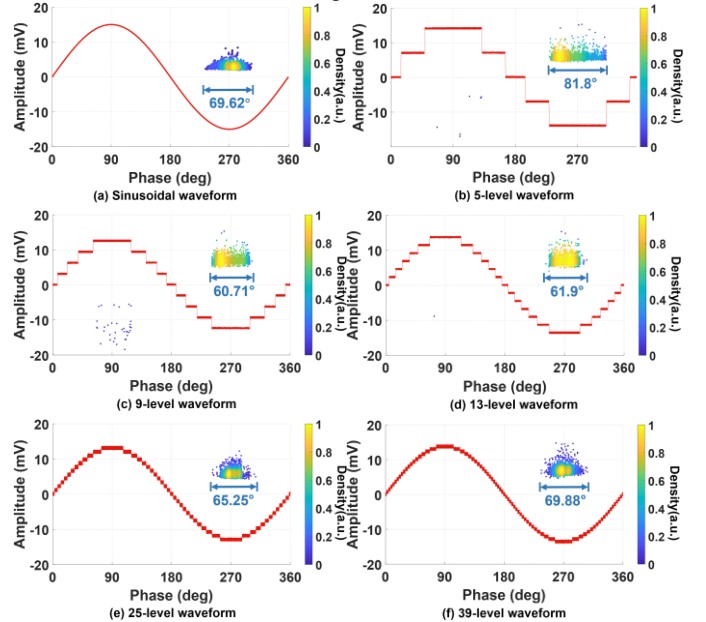


Fig. 3. PRPD patterns of the needle defect under different waveforms (voltage peak 14kV).

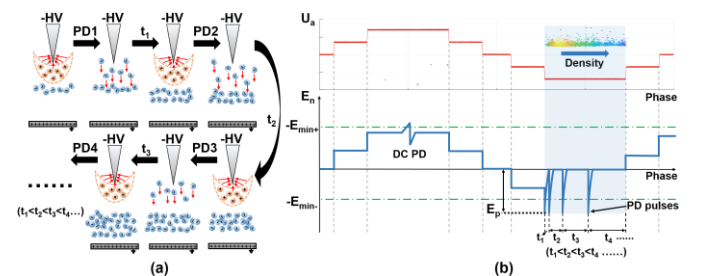


Fig. 4. (a) Electron accumulation process of negative corona discharge. (b) External applied voltage (U_a) and resultant electric field inside the needle defect (E_n) as function of phase for 5-level staircase waveform. t_n represents the time interval between two consecutive PDs.

B. Floating defect

In Fig. 5, it can be seen from the PRPD patterns of the floating defect under the sinusoidal waveform, 5-, 9-, 25-, 39- and 79-level staircase waveform that the PD phase distribution shows a significant correlation with the step change. Although this phenomenon is typical for PD at staircase voltages, the overall shape of the PRPD patterns when the staircase voltage is applied to the floating defect differs significantly from existing studies [4, 13]. Since the PD process under 5-level staircase waveform is more representative, this article uses it as an example to illustrate the difference between the discharge process of the floating defect at staircase voltage and at sinusoidal voltage, as shown in Fig. 6.

In Fig. 6(a), there is a hysteresis regarding the electric field recovery of the PD. Since the electrode is floating and is mostly covered with gas (except the support insulator underneath it) the charges on the floating electrodes after each PD cannot decay quickly, because of high resistance seen by the floating electrodes (large time constant). This causes the hysteresis of the electric field recovery. Moreover, this also makes the time interval between the two discharges longer, resulting in less discharges in the DC stage of the staircase waveform. In the meantime, the remaining charges generate a background electric field opposite to the applied voltage between the floating electrodes, which weakens the discharge excitation electric field in the defect. This means that the next discharge requires a higher applied voltage to meet the PD inception electric field, and less likely produce PD at the same voltage in the DC stage. Thus, the PD is mainly concentrated on the rising edge of the staircase waveform.

According to the electric field change of the floating discharge, the overall PD mainly includes four stages. Fig. 6(a) shows the positions of the four stages in the whole cycle, and Fig. 6(b) shows the discharge mechanism of each stage in detail. The first stage is that the PD occurs at the positive DC component of the staircase waveform, at which time the floating defect is in a state of electric field balance. Due to the background field, the floating objects get a floating potential, and hence there can be an electric field between HV and floating electrode as well as between floating electrode and ground. The second stage is that after the PD occurs in the positive half-cycle, which corresponds to transient phase after the voltage step of the staircase waveform. This is because floating object is a metal, the top side of it which is in front of the positive electrode can have an induced negative charge and its lower part will get induced positive charge (their sum is zero). When there is a PD, those negative charges from the top side of the floating metal can move to the positive electrode. The fact is that space charges are not left in the gap, which actually disappear after around 50 μ s. The charges will be left on the surface of floating electrode and their electric field will oppose the background field. The third stage is the DC component phase where the staircase waveform is in the negative half-cycle.

As the magnitude of the applied voltage decreases from the positive value to zero and negative, the background field due to the applied voltage decreases and changes its direction. Since the electric field due to charges on the floating object still keep their direction, the reduction and gradual change of direction of the electric field due to applied voltage, results in an overall electric field in the gap to exceed the PD inception voltage. Hence, we have observed the next discharge. The fourth stage is in the transient stage after the PD occurs in the negative half-cycle of the staircase waveform. The positive charges in the defect gap are transferred to the cathode. A large number of negative charges left in the gap dominate the electrostatic field, preventing the recurrence of the PD in a short time. Based on this, it can be found that when the sinusoidal and the staircase waveforms are close to the polarity conversion, the resultant electric field is more likely to produce PD, which is why the floating discharge mainly starts from 0° and 180° .

For the shape details of these PRPD pattern, as the number of levels increases, the spacing between PD clusters gradually decreases, and its overall shape tends to be the sinusoidal distribution. In Fig. 5(b) and Fig. 5(c), it also can be seen from the partial enlarged view of the patterns under the staircase waveform that there is basically a “tail” behind each PD cluster. The formation of this “tail” is caused by the statistical time lag of PD. The time lag is caused by the unavailability of free electrons to initiate an electron avalanche after the internal electric field of the defect has reached the conditions required for PD, which explains the PD appearance delay [20]. The probability for a single electron to initiate an electron avalanche is:

$$P(E_a) = 1 - \eta(E_a)/\alpha(E_a) \quad (3)$$

where η is the electron attachment rate, α is the electron ionization rate, and both of them are related to the external electric field E_a .

The generation rate of the electron is:

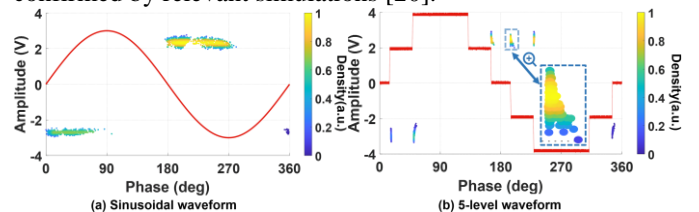
$$N(E_a) = N_0 + N_e(E_a) + N_d(E_a) \quad (4)$$

where N_0 is the electron change rate of the background ionization, N_e is the electron change rate of the field emission, and N_d is the electron rate of the detachment.

According to (3) and (4), the generation rate of the effective electron is:

$$\frac{dN(E_a)}{dt} = \int_S P(E_a)N_e(E_a)ds + \int_V P(E_a)[N_d(E_a) + N_0]dv \quad (5)$$

where S is surface of the electrode region, V is the volume of the defect gap. The process of the time lag can be expressed as the generation rate of the effective electron. Based on the above analysis, we believe that the tail-like distribution of the PRPD pattern is caused by the PD time lag, and this principle has been confirmed by relevant simulations [20].



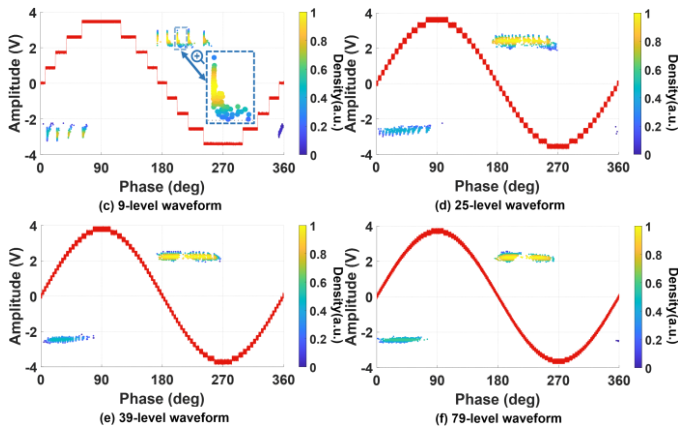
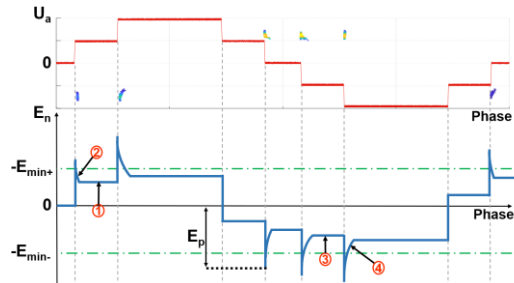
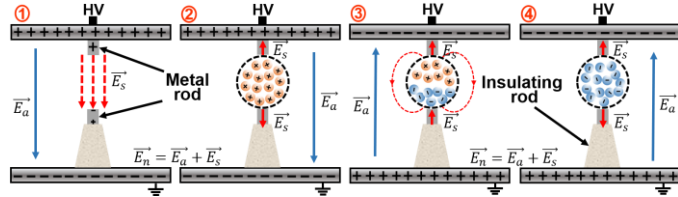


Fig. 5. PRPD patterns of the floating defect under different waveforms (voltage peak 13kV).



(a) External applied voltage (U_a) and electric field inside the floating defect (E_n) as function of phase for 5-level staircase waveform.



(b) The four main electric field distribution states of the floating defect under the staircase waveform. 1, 2 are the positive half-cycle states, and 3, 4 are the negative half-cycle states, respectively corresponding to the serial numbers in Fig. 6(a).

Fig. 6. PD process of floating defect under 5-level staircase waveform.

C. Particle defect

For the particle defect, the PRPD pattern under 5-, 9-, 13-, 39-, 59- and sine waveform are selected for analysis and are shown in Fig. 7. It can be seen that the particle PD is distributed in two clusters of “rabbit ears” under positive and negative amplitudes under sinusoidal waveform. The formation of “rabbit ears” is the result of the joint effect of the PD generated conditions and the electronegative molecules [21]. However, the shape of the “rabbit ears” changed under the staircase voltage compared to the shape under the sinusoidal voltage. The difference is that PRPD patterns show a stripe-like clustering distribution while maintaining almost a similar contour of the “rabbit ears” under staircase voltage. The phase position of the stripe-like distribution corresponds to the step change of the staircase waveform, where a jump change of each voltage level causes a cluster of strip discharge. The interval between stripes shortens as the level rises, and gradually becomes evenly distributed. It can be seen from Fig. 7(e) that the PRPD pattern

under 59-level staircase waveform is basically the same as the sine based on visual observation.

Because the particle discharge under staircase-based sinusoidal voltage contains a variety of complex motion processes, it has great randomness. These motion statuses are difficult to accurately determine. At present, there is no research to analyze particle motion state based on the staircase waveform. Therefore, this paper selects 5 typical states in the particles discharge process to illustrate its PD behavior under the staircase waveform.

State 1: A free particle with mass m is at the critical movement, shown in the green number 1 in Fig. 8. At this time, the particle is mainly affected by the electrostatic field force F_e and gravity mg . The critical lifting state can be expressed [22] as:

$$F_e = E_a q = \frac{U}{d} \cdot \frac{2\pi^3 \epsilon r^2 U}{3d} \geq mg \quad (6)$$

where E_a : external electric field, q : charge, U : applied voltage, ϵ : dielectric constant, d : distance between the electrodes, r : radius of a sphere, g : gravitational field.

In this state, since the initial velocity of the particle is zero, discharge will only occur when the voltage of the staircase waveform rises to meet (6). When the particles are lifted by the force of the electric field, they will be discharged when they contact the electrode plate again, which is one of the reasons that there are more discharges distributed on the rising edge of the staircase waveform.

State 2: The force of the external electric field F_e increases when the particle moves in the same direction as the F_e , as shown in Fig. 8 as number 2 with green. The particle is suspended in the gas at this state, mainly subject to F_e , mg and the drag force F_d . Since the particle is very small and the distance between the plates is very short, the influence of the drag force can be ignored in this condition [23], the force relationship can be shown as follows:

$$F_e - mg = m \frac{d\bar{v}}{dt} \quad (7)$$

where v is the particle velocity, and it is defined that the upward direction perpendicular to the plate is positive.

Whenever a particle leaves the electrode to the next discharge, the charge q carried on the particle can be regarded as constant. Therefore, when experiencing a steep rising edge in the staircase waveform, the electric field force F_e will suddenly increase. According to (7), the particle can have a higher acceleration, so as to increase the probability of particles touching the electrode when the voltage changes suddenly, which is also one of the reasons why the discharge is more distributed along the rising edge of the staircase waveform.

State 3: The force of the external electric field F_e decreases when the particle moves in the same direction as F_e , as shown in Fig. 8 as number 3 with green. This state corresponds to the falling edge of the staircase waveform. The particle has the same charge as the upper plate after the rebound from the upper plate, which satisfies (8).

$$-F_e - mg = m \frac{d\bar{v}}{dt} \quad (8)$$

When the applied voltage drops, the acceleration of the dropping particle decreases, thereby delaying the time to reach

the lower plate. This stage is one of the reasons for the random discharge in the interval of the stripes.

State 4: The movement direction of the particle is opposite to the external electric field force, shown in the green number 4 in Fig. 8. When the particle has lifted off and suspended in the gap, the change in the polarity of the staircase-based sinusoidal voltage will cause this state. This state mostly appears at the rising edge after the phase distribution of 0° and 180° . There are two situations possible, namely, the voltage polarity changes during the rising or falling of the particles. These two situations are not only the reason for the stripe-like distribution, but also the reason for the random discharge between the stripes.

State 5: The particle discharge under a uniform electric field in the DC component stage of staircase waveform. Because the DC component has a constant amplitude, whether it can lift off depends on the voltage amplitude reached by the previous rising or falling edge. In addition, when the particle is in the active state after the last PD, it may continue to produce the next discharge under the DC component state. This state is one of the main reasons for the scattered discharge in the interval of the stripe-like distribution.

Since the basic simulation theory of particle discharge is still applicable at staircase voltage, the difference is that we have divided the particle discharge at staircase voltage into 5 states. Under the combined action of these five main speculations of discharge processes, the PD presents a stripe-like distribution corresponding to the staircase, but at the same time it also has a rough outline like the sinusoidal discharge.

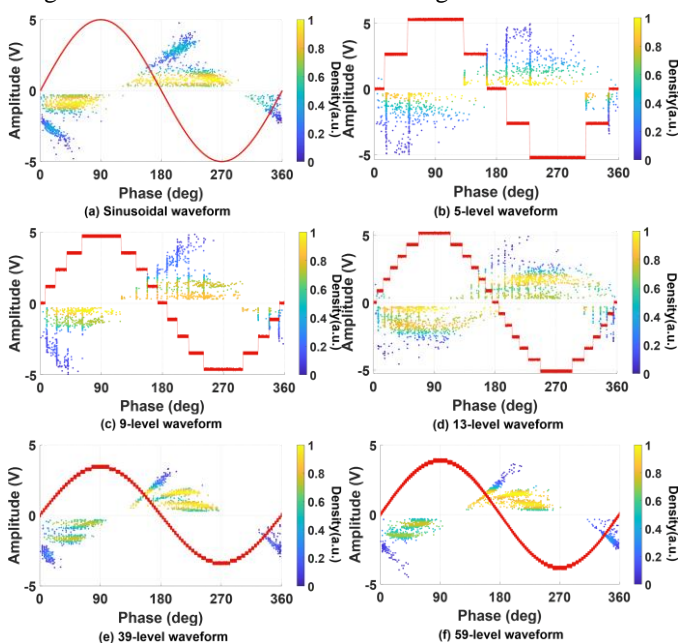


Fig. 7. PRPD patterns of the particle defect under different waveforms (voltage peak 17kV).

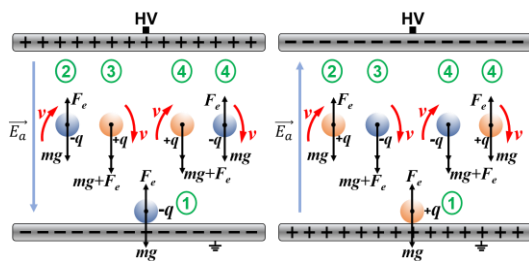


Fig. 8. Four typical states of particle discharge under staircase waveform.

D. Surface defect

Fig. 9 shows the PRPD pattern of the surface defect under the sine wave, 5-, 9-, 13-, 25-, and 39-level staircase waveform. For the staircase waveform, there is a clear stripe-like distribution near the voltage step, which is a similar phenomenon that has been found in some current studies [4, 13]. However, the difference is that the discharge only occurs at the rising edge of (absolute value of voltage) the staircase waveform at 5-level and 9-level, and a small amount of discharge begins to appear at the falling edge (absolute value of voltage) at 13-level, 25-level and 35-level. This is because when the number of levels is low, the voltage change of a step drop is large, which causes the first falling edge after the peak to be insufficient to support the generation of PD. When the staircase waveform reaches 39-level, the stripe-like distribution almost disappears.

The surface discharge process is almost similar to the discharge of floating defects in Fig. 6(a), both of which are PD with dielectric barriers, but the specific conditions for PD generation are different due to different dielectric structures. In particular, the discharge amplitude of surface discharge in the positive half cycle is relatively lower than that in the negative half cycle, which is related to the structure of electrodes. Since the field strength near the high-voltage electrode is high, the surface PD is generated on the interface of the high-voltage electrode and the dielectrics. In addition, because the dielectrics blocks the emission of electrons from the ground electrode to a certain extent, it is easier to emit electrons when the high-voltage electrode is negative, and at the same time, positive ions hit the cathode to cause secondary electron emission, resulting in greater discharge.

In addition, from Fig. 9(b) and (c), it is found that surface discharge also has a time lag similar to that of floating discharge, forming a “tail”. The principle of time lag in the surface defect can also be explained by (3) to (5). It is worth noting that the shape of the tail has a higher amplitude at the head and a lower amplitude at the end of the tail. This is because the first PD after the rising edge can cause the space charges attached to the surface of dielectric. As the number of PD increases, the accumulation of space charges will weaken the electric field on the surface of the defect. Therefore, in the DC stage of the same voltage, the resultant electric field that generates PD becomes smaller, resulting in a gradual decrease in the discharge amplitude.

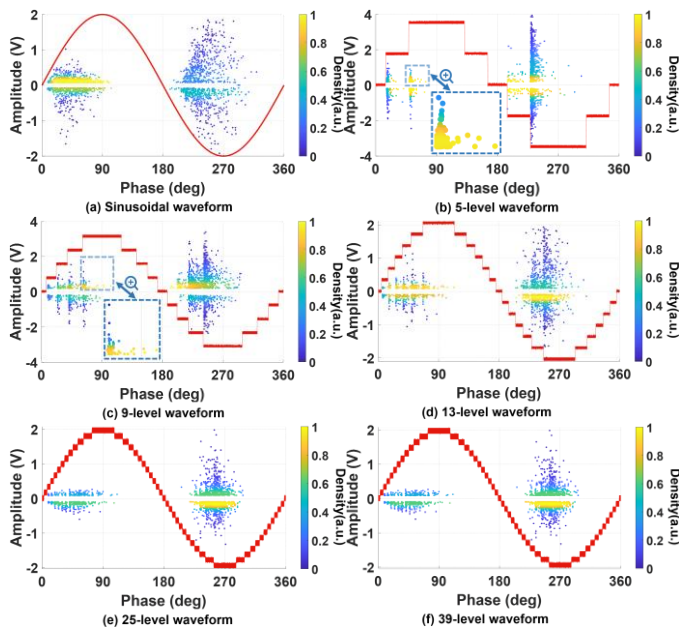


Fig. 9. PRPD patterns of the surface defect under different waveforms (voltage peak 25kV).

E. Internal defect

Internal defect is a kind of PD defect that is common in various power equipment, which indicates the presence of air bubbles in the insulating material. Fig. 10 shows the PRPD patterns of internal defects under different waveforms. Under the sinusoidal and staircase waveform, the distribution of positive and negative half cycles is basically symmetrical.

The distribution of PD at the changing edge of the square voltage is also observed in previous work, which is still applicable in the staircase voltage, except that the PD amplitude differs at different levels of the staircase voltage [24]. When the number of levels increases, the overvoltage after each voltage step is not that large and so the magnitude of PDs are smaller [15]. In the DC stage of staircase voltage, we can get only very few PD during DC stage, but the magnitude of PDs near the edge are the largest among all cases, which might be caused by the time lag.

In order to investigate more fully the PD behavior of an internal void under staircase voltage, we have built a numerical simulation model in Simulink for the internal void PD under staircase waveform. Based on a typical *abc* capacitor equivalent circuit with internal void PD, its numerical simulation model is built in Simulink as shown in Fig. 11. In the simulation, the semi-conductivity of the void surface occurs during the PD process is considered. When the voltage through the void reaches the PD inception voltage, the insulation resistance R_2 along the void surface is instantaneously reduced to its corresponding semi-conducting resistance R_{22} . The voltage source is a 50Hz 5-level staircase voltage of 5kV peak value. The equivalent capacitance $C_a=0.7\text{pF}$, $C_b=0.04\text{pF}$, $C_c=0.06\text{pF}$. Void resistance R_1 is $2 \times 10^{10} \Omega$. Void surface resistance R_2 is $6 \times 10^{10} \Omega$. Void semiconducting resistance R_{22} is $8 \times 10^5 \Omega$. The excitation of the PD is controlled by a switch in the simulation. The distribution diagram of the internal void

voltage and PD current pulses in one cycle is obtained by simulation in Fig. 13.

From Fig. 12, PDs occur at the rising or falling edge of the staircase voltage, which fits well with the experimental results and the supporting assumptions. However, by comparing the experimental PRPD patterns with the simulation results, we can see that the PD pulses are concentrated at the changing edge of the staircase voltage when no time lag is set in the simulation, while in the PRPD patterns the PDs appear in the DC part of the staircase voltage, which indicates that the time lag phenomenon does exist in the internal discharge at the real staircase voltage [24].

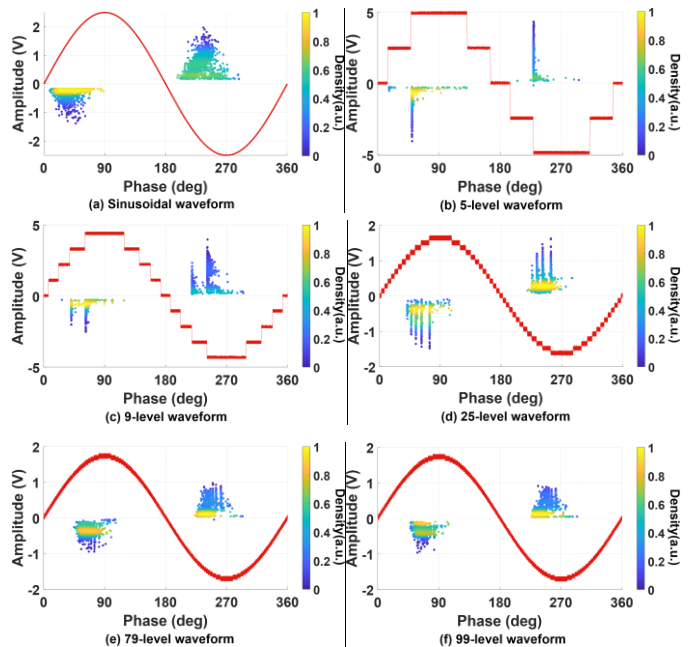


Fig. 10. PRPD patterns of the internal defect under different waveforms (voltage peak 15kV).

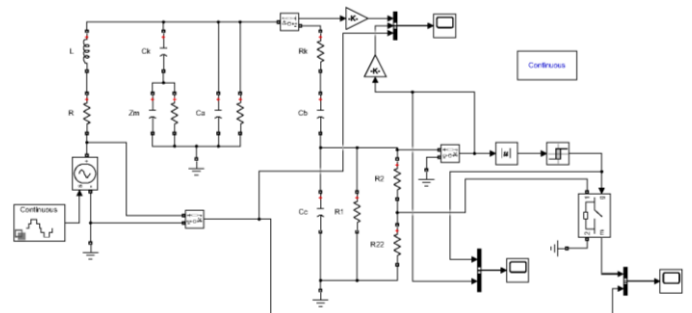


Fig. 11. Numerical simulation model of the internal void PD.

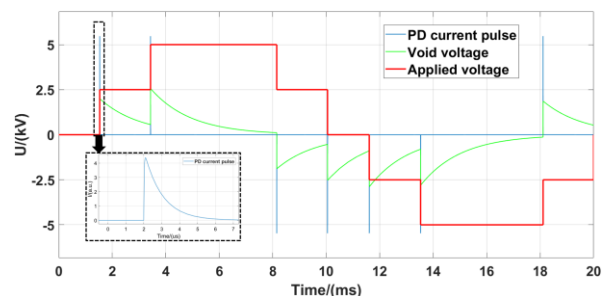


Fig. 12. Distribution diagram of the voltage through the internal void and PD current pulses in one cycle.

F. PRPD pattern similarity analysis

Since the previous sections only visually compares the similarity of the PD patterns under the staircase voltage and the sinusoidal voltage, it cannot reflect the specific details of the distribution scientifically and accurately. Therefore, in order to compare the changes of the PRPD pattern under the staircase waveform and the sinusoidal waveform in a more detailed and quantitative manner, this paper proposes the concept of average phase similarity (APS).

For a PD defect, APS is defined as the difference in the number of discharges per degree of phase between the PRPD pattern under non-sinusoidal voltage and that under sinusoidal voltage. It can be expressed as:

$$APS = \text{mean}(|N_a(d) - N_b(d)|), \quad 0 \leq d \leq 360 \quad (9)$$

where $N_a(d)$ is the number of discharges in d degree of phase under a non-sinusoidal waveform, $N_b(d)$ is the number of discharges in d degree of phase under a sine waveform, and d is the phase degree. The larger the value of APS, the greater the difference between the test pattern and the pattern under the sinusoidal waveform, and 0 means the totally same. However, due to the instability of PD, it is difficult to make APS equal to zero even with two patterns under the same condition. Therefore, it is unreasonable to regard APS=0 as the criterion. Since different defects have different discharge rules and randomness, the APS reference standard for each defect is proposed in Table I. This reference standard is to conduct 10 experiments on the same defect under the same conditions. One of the PRPD patterns is selected as the reference pattern, and the average APS of the remaining 9 patterns relative to the reference pattern is calculated, which can obtain the APS reference standard under each defect. This means that when the APS reaches the value of the reference standard, these two patterns can be considered the same. Fig. 13 shows the APS of 5 kinds of defects under different staircase waveform.

It can be seen from Fig. 13 that the overall trend of the APS of all defects decreases as the number of levels increases, which means that they are all gradually become similar to the pattern under the sinusoidal waveform. When the number of levels is low, the APS of the floating defect is the highest, and the APS of the needle defect is the lowest. As the number of levels increase, the APS value of the internal defect becomes the highest, while the amount of the needle defect remains the lowest. Furthermore, the APS of the floating defect has the largest variation, which means that it is more susceptible to changes in the number of levels. Comparing the APS of each defect at 99-level with the reference standard, it can be assessed that the PRPD pattern of the particle defect has the highest similarity (closest to the reference line in Fig. 13), indicating that the range of influence by the level of the staircase waveform is relatively small. The APS of internal defects is generally higher than the other defects, indicating that the internal defect discharge is more sensitive to the staircase waveform, and a higher level is required to be equivalent to the discharge under the sinusoidal waveform. This may be caused by the enclosed space of internal defects and the existence of space charges that were not neutralized in the previous

discharge. There is no accumulation of space charges for particle defects through the exchange of charges by metal particles, which makes particle defects less responsive to level changes.

Through the analysis of APS, it is found that different defects have different response degrees to the staircase waveform. Moreover, another important finding is that even when the level number reaches 99-levels, the APS under staircase voltage is still different from the APS under the sinusoidal voltage. These findings provide an important theoretical reference for the PD behavior under multi-level voltage and the development of arbitrary waveform high-voltage test sources.

TABLE I
APS REFERENCE STANDARDS WITH DIFFERENT DEFECTS

Defect	Needle	Floating	Particle	Surface	Internal
APS (deg/pulses)	0.47	1.20	2.44	1.41	3.35

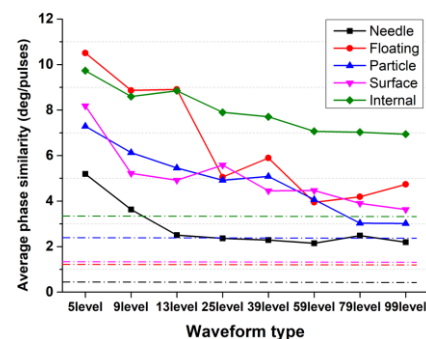


Fig. 13. APS of 5 kinds of defects under different waveforms. The colored dotted lines indicate the APS reference standard.

IV. THE EFFECT OF SLOPE OF STEP RESPONSE ON PD BEHAVIOR

In order to study the influence of the step response of the staircase waveform on the PD behavior, the work in this paper increases the value of the coupling capacitor to slow down the step response of the staircase waveform, which results in a voltage gradient down to about $8V/\mu s$. Although the staircase voltage with such a slow voltage gradient will not occur in practice, this can provide a theoretical reference for the effect of voltage gradient variations on PD behavior. Therefore, in order to more clearly reflect the effect of slowing down the voltage gradient on the PD, an extremely slow voltage gradient is used in this paper to equivalently reveal the microscopic changes.

Through the analysis in Section III, the five typical defects mainly present three distribution states under the staircase waveform, which are square-like, tail-like and stripe-like distributions. Therefore, 3 defects that can represent 3 typical distribution states are used to study the effect of step response on PD behavior. In order to show the changes brought about by the step response more clearly, this article takes the 5-level staircase waveform as an example for illustration, as shown in Fig. 14.

It can be seen from Fig. 14 that the slowing of the step response brings different changes to the PRPD patterns of different defects. For the square-like distribution of the needle defect, the low-slope rising edge expands its distribution range

from 81.8° to 87.12° . Also, the distribution of squares becomes less obvious. For the tail-like floating defect, the head of the tail becomes gradually smooth and uniform, and the tail gradually becomes longer. For the stripe-like particle defect, it can be seen that the stripes have become wider by contrast, but they still start from the stair edge. By comparing the PRPD patterns of the three typical defects at fast and slow voltage gradients, basically the PD phase distribution range at the voltage step edge becomes wider by about 6° , which is basically consistent with the longer voltage step time.

Synthesizing the change trend of the three typical distributions, it can be found that the PD is still distributed along the voltage step edge of the staircase waveform in the case of a slow step response, which is similar to the distribution at the high voltage gradient. This indicates that the PD mechanism at high voltage gradients still works at the low voltage gradient. Therefore, the phase range to satisfy the PD condition becomes wider when the amplitude of each level of the staircase voltage remains the same and the voltage step time becomes longer. As a result, the phase distribution of the PD at the voltage step edge of the PRPD pattern at the low voltage gradient becomes wider.

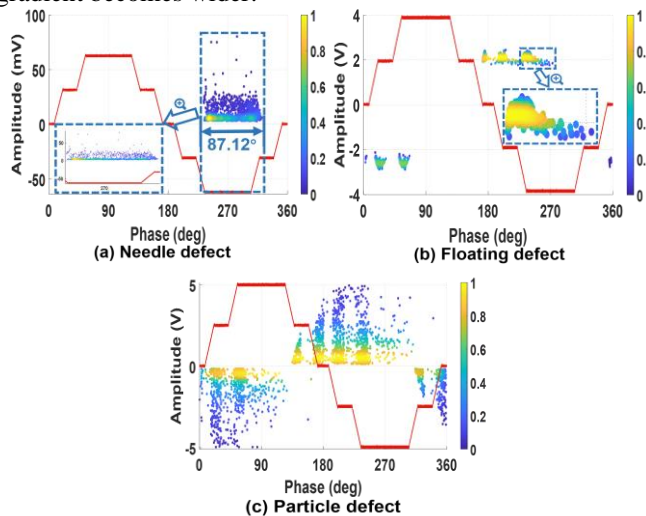


Fig. 14. PRPD patterns of three defects under slow-slope staircase waveform.

V. PD PULSE REPETITION RATE

In order to study the influence of different waveforms on the PRR of PD, the experiments on 5 typical defects under 5-, 9-, 13-, 25-, 39-, 59-, 79-level staircase waveforms and the sinusoidal waveform are conducted in this paper, as shown in Fig. 16. We found in our experiments that the change in voltage gradient does not have a significant effect on the PRR, and this phenomenon was also confirmed in the reference [25]. Therefore, we focus on the PRR of PD under the fast voltage gradient in this paper.

On the whole, the PRR of the needle defect is the highest under each waveform, while the PRR of the surface discharge is basically the lowest. According to specific results, the PRR of the needle defect decreases with the increase of the number of levels, and the PRR under sinusoidal waveform is the lowest. For the particle defect, PRR fluctuates under different levels of

staircase waveforms, which is due to the strong randomness of the particle discharge. However, it can be roughly seen that the overall change trend of PRR decreases as the number of levels increases. The PRR of floating discharge is relatively stable, and it remains at about 110 pulses/s under the staircase waveforms and the sine waveform, which shows that the PRR of the floating discharge is not sensitive to the number of waveform levels. Regarding the surface defect, the PRR of the surface defect also decreases with the increase of the number of levels, and the PRR under sine waveform is the lowest. However, the decrease change in PRR of surface defects is smaller than that of needle defects. The PRR of the surface defect reduces from 111 pulses/s to 33 pulses/s, while that of the needle defect reduces from 2500 pulses/s to 641 pulses/s. Unlike other defects, the PRR of the internal defect tends to decrease first and then starts to increase with the increase of the levels of the staircase waveform, which are all lower than the PRR under the sine waveform for the internal defect.

According to the results of different defects in different waveforms, the PD under the staircase waveform will cause changes in PRR, which can have an important impact on the aging and discharge of the power equipment insulation. Therefore, the diagnosis of PD under new electrical stress needs to be considered carefully.

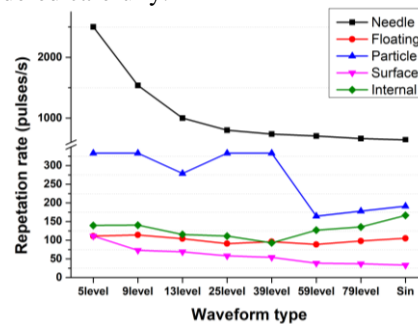


Fig. 15. Pulse repetition rate of 5 kinds of defects under different waveforms.

VI. CONCLUSIONS

In this paper, PD behavior of 5 typical defects is studied for staircase voltage with different number of levels and traditional sinusoidal voltage. Since the staircase waveform is a new electrical stress for power equipment, following four important aspects are observed:

(1) Different defects have different sensitivity to the staircase waveform. The PRPD patterns of the needle defect, floating defect, particle defect, surface defect and internal defect are visually close to that of the sinusoidal waveform under the 39-level, 79-level, 59-level, 39-level and 99-level staircase waveforms respectively in visual. However, for the distribution details of the PRPD pattern, even all defects at 99-level staircase waveform still have differences from the pattern under sinusoidal waveform. APS results show that the internal defect is the most sensitive to the staircase waveform, which indicates that the internal defect is easier to suffer from the new electrical stress. The particle defect is the least sensitive to staircase waveforms. When new electrical stresses of different levels appear on the equipment, this work not only provides an

important reference for whether the traditional sinusoidal PRPD information can be used for future on-site PD detection, but also it serves as a guideline for development of new power electronics based high-voltage test sources, such that its impact on insulation material during testing is the same as for traditional test source when the test waveform is a sinusoidal waveform.

(2) Different defects have different responses under the staircase waveform. The influence of the staircase waveform on the needle defect is the change of the PD phase distribution width, and appears the square shape distribution. The floating discharge presents a tail-like cluster distribution corresponding to the step edge under the staircase waveform. Regarding the particle defect under the staircase waveform, in the PRPD distribution not only a stripe-like distribution appears, but also it keeps roughly the same profile as the sinusoidal PRPD pattern. The surface discharge and internal discharge both have obvious correlation with the staircase, forming a tail-like distribution at each level. In addition, when the step response of the staircase waveform becomes slower, the PD phase distribution near the voltage step edge becomes wider. Since the PRPD pattern under the staircase waveform is different from that of the sine waveform, the research in this article provides the explanation which can be used for PD diagnostics and mechanism of PD patterns originated from different defects.

(3) The staircase waveform can affect the PD pulse repetition rate of different defects. With the increase in the number of staircase waveform levels, the PRR of the needle defect and surface defect decreases, and the drop of the needle defect is the largest. Similarly, the PRR of the particle defect also shows a downward trend with some fluctuations. On the contrary, the PRR of the internal defect under the staircase waveform is lower than that of under the sine waveform. Differently, the PRR of the floating defect is almost not affected by the level change of the staircase waveform, and is almost the same as that of the sine. Therefore, the staircase waveform can make a certain change in PRR, which means that the influence of the staircase waveform on the aging and discharge hazards of the insulation needs to be considered.

(4) Due to the typicality of these five types of defects, and the detailed explanation of the difference between PD phenomena under staircase waveform and sinusoidal waveform, the results not only show the PD behavior under the staircase waveform listed in this article, but can also be used to analyze the PD phenomenon and test under other similar step voltages.

REFERENCE

- [1] J. P. Contreras, and J. M. Ramirez, "Multi-fed power electronic transformer for use in modern distribution systems," *IEEE Trans. Smart Grid*, vol. 5, no. 3, pp. 1532-1541, 2014.
- [2] N. Prabaharan, K. Palanisamy, "A comprehensive review on reduced switch multilevel inverter topologies, modulation techniques and applications," *Renew. Sust. Energ. Rev.*, vol. 76, pp. 1248-1282, 2017.
- [3] P. Lei, Y. Mingtian, L. Geqi, *et al.*, "A high voltage multi level arbitrary waveform generator for insulation testing," *IEEE Trans. Dielectr. Electr. Insul.*, vol. 26, no. 2, pp. 405-411, 2019.
- [4] M. Florkowski, P. Błaszczyk, P. Klimczak, "Partial discharges in twisted-pair magnet wires subject to multilevel PWM pulses," *IEEE Trans. Dielectr. Electr. Insul.*, vol. 24, no. 4, pp. 2203-2210, 2017.
- [5] Y. Zang, Y. Qian, H. Wang, *et al.*, "A Novel Optical Localization Method for Partial Discharge Source Using ANFIS Virtual Sensors and Simulation Fingerprint in GIL," *IEEE Trans. Instrum. Meas.*, vol. 70, pp. 1-11, 2021.
- [6] R. Piccin, A. R. Mor, P. Morshuis, *et al.*, "Partial discharge analysis of gas insulated systems at high voltage AC and DC" *IEEE Trans. Dielectr. Electr. Insul.*, vol. 22, no. 1, pp. 218-228, 2015.
- [7] M. Florkowski, "Influence of high voltage harmonics on partial discharge patterns," in *Proceedings of 5th International Conference on Properties and Applications of Dielectric Materials, SEOUL, SOUTH KOREA*, vol. 1, pp. 303-306, 1997.
- [8] K. Wu, T. Okamoto and Y. Suzuoki, "Effects of discharge area and surface conductivity on partial discharge behavior in voids under square voltages," *IEEE Trans. Dielectr. Electr. Insul.*, vol. 14, no. 2, pp. 461-470, 2007.
- [9] H. A. Illias *et al.*, "Simulation of partial discharge within a void under square waveform applied voltage," *Annual Report Conference on Electrical Insulation and Dielectric Phenomena, Montreal, Canada*, pp. 76-79, 2012.
- [10] H. Okubo, N. Hayakawa, G. C. Montanari, "Technical development on partial discharge measurement and electrical insulation techniques for low voltage motors driven by voltage inverters," *IEEE Trans. Dielectr. Electr. Insul.*, vol. 14, no. 6, pp. 1516-1530, 2007.
- [11] G. C. Montanari, "Time behavior of partial discharges and life of type II turn insulation specimens under repetitive impulse and sinusoidal waveforms," *IEEE Electr. Insul. Mag.*, vol. 33, no. 6, pp. 17-26, 2017.
- [12] H. You, Z. Wei, B. Hu, *et al.*, "Partial Discharge Behaviors in Power Modules Under Square Pulses With Ultrafast dv/dt," *IEEE Trans. Power Electron.*, vol. 36, no. 3, pp. 2611-2620, 2020.
- [13] P. Wang, A. Cavallini, G. C. Montanari, "Characteristics of PD under square wave voltages and their influence on motor insulation endurance," *IEEE Trans. Dielectr. Electr. Insul.*, vol. 22, no. 6, pp. 3079-3086, 2015.
- [14] L. Benmamas, P. Teste, E. Odic, *et al.*, "Contribution to the analysis of PWM inverter parameters influence on the partial discharge inception voltage," *IEEE Trans. Dielectr. Electr. Insul.*, vol. 26, no. 1, pp. 146-152, 2019.
- [15] P. Seri, G. C. Montanari, R. Hebner, "Partial discharge phase and amplitude distribution and life of insulation systems fed with multilevel inverters," in *2019 IEEE Transportation Electrification Conference and Expo (ITEC), Novi, MI, 2019*, pp. 1-6.
- [16] G. Li, H. Liu, T. Long, *et al.*, "Development of High Voltage Multilevel Step-wave Voltage Source," in *2018 IEEE International Power Modulator and High Voltage Conference (IPMHVC), Jackson, WY, 2018*, pp. 339-343.
- [17] D. A. Ganeshpure, T. B. Soeiro, M. G. Niasar, *et al.*, "Modular Multilevel Converter-based Arbitrary Wave shape Generator used for High Voltage Testing," in *2021 IEEE 19th International Power Electronics and Motion Control Conference (PEMC), Silesian Univ Technol, ELECTRONETWORK, 2021*, pp. 124-131.
- [18] P. Wang, A. Cavallini, G. C. Montanari and G. Wu, "Effect of rise time on PD pulse features under repetitive square wave voltages," *IEEE Trans. Dielectr. Electr. Insul.*, vol. 20, no. 1, pp. 245-254, 2013.
- [19] P. H. F. Morshuis, J. J. Smit, "Partial discharges at DC voltage: their mechanism, detection and analysis," *IEEE Trans. Dielectr. Electr. Insul.*, vol. 12, no. 2, pp. 328-340, 2005.
- [20] P. Fu, Z. Zhao, X. Li, *et al.*, "The role of time-lag in the surface discharge inception under positive repetitive pulse voltage," *Phys. Plasmas*, vol. 25, no. 9, pp. 093518, 2018.
- [21] K. Wu, F. Komori and Y. Suzuoki, "Effects of oxygen on the formation of rabbit-like PD pattern in a void between metal surfaces," *Proceedings of 2001 International Symposium on Electrical Insulating Materials (ISEIM 2001). 2001 Asian Conference on Electrical Insulating Diagnosis (ACEID 2001). 33rd Symposium on Electrical and Ele*, pp. 37-40, 2001.
- [22] K. Asano, K. Yatsuzuka, Y. Higashiyama, "The motion of charged metal particles within parallel and tilted electrodes," *J. Electrostat.*, vol. 30, pp. 65-74, 1993.
- [23] M. M. Morcos, H. I. Anis, K. D. Srivastava, "Metallic particle movement, corona, and breakdown in compressed gas insulated transmission line systems," *IEEE Trans. Ind. Appl.*, vol. 27, no. 5, pp. 816-823, 1991.
- [24] C. Pan, G. Chen, J. Tang and K. Wu, "Numerical modeling of partial discharges in a solid dielectric-bounded cavity: A review," *IEEE Trans. Dielectr. Electr. Insul.*, vol. 26, no. 3, pp. 981-1000, 2019.
- [25] D. A. Ganeshpure, L. C. C. Heredia, M. G. Niasar, *et al.*, "Analysis of Partial Discharge Behaviour under Staircase-based Sinusoidal Voltage Waveforms," *IEEE 3rd International Conference on Dielectrics (ICD), Valencia, SPAIN*, pp. 894-897, 2020.